

Fractal dimension of steady nonequilibrium flows

William G. Hoover

Department of Applied Science, Post Office Box 808, University of California at Davis-Livermore, California 94550

Harald A. Posch

Institute for Experimental Physics, Boltzmanngasse 5, University of Vienna, Vienna A-1090, Austria

Carol G. Hoover

Methods Development Group, Mechanical Engineering Department, Lawrence Livermore National Laboratory, Livermore, California 94550

(Received 20 September 1991; accepted for publication 25 February 1992)

The Kaplan–Yorke information dimension of phase-space attractors for two kinds of steady nonequilibrium many-body flows is evaluated. In both cases a set of Newtonian particles is considered which interacts with boundary particles. Time-averaged boundary temperatures are imposed by Nosé–Hoover thermostat forces. For both kinds of nonequilibrium systems, it is demonstrated numerically that external isothermal boundaries can drive the otherwise purely Newtonian flow onto a *multifractal attractor* with a phase-space information dimension significantly less than that of the corresponding equilibrium flow. Thus the Gibbs' entropy of such nonequilibrium flows can diverge.

I. INTRODUCTION

It has been demonstrated, both theoretically and numerically, that nonequilibrium steady states of classical many-body systems can inhabit multifractal phase-space attractors.^{1–5} Both kinds of demonstrations make use of Nosé–Hoover canonical thermostats to impose thermal constraints on selected boundary degrees of freedom. These boundary degrees of freedom play the role of thermodynamic thermostats by imposing a time-averaged boundary temperature $T \equiv \langle p^2/mk \rangle$ on each boundary degree of freedom. The *theoretical* approach^{1–3} to establishing fractal behavior begins with the Liouville equation and ends with the result that Gibbs' many-body probability density $f_N(q_N, p_N, \xi)$ *diverges* for any such nonequilibrium steady state. The alternative *numerical* approach confirms this theoretically predicted divergence. For systems with only a few phase-space dimensions the multifractal nature of the probability density^{1–5} is evident in numerically generated phase-space cross sections, called “Poincaré sections.”

The new deterministic time-reversible Nosé–Hoover thermostats used to establish these surprising facts replace the more traditional stochastic boundaries familiar from the Langevin equation.⁶ Because the classical Langevin approach cannot be used to analyze phase-space structure, the new results have piqued considerable interest and have also generated some sceptical criticism. Eyink and Lebowitz have emphasized to us that special stochastic “boundary” conditions can lead to a continuous nonfractal phase-space measure.⁷ Evidently, the assumption of stochasticity can smear out the fractal measure that we obtain in the present work by using time-reversible deterministic equations of motion. The sceptics feel, based on these rigorous results for the simpler, stochastic models, that nonequilibrium steady-state phase-space distribution functions may

not, in fact, be fractal so that Gibbs' entropy could still be a useful concept away from equilibrium.⁷

The theoretical analysis of the Nosé–Hoover isothermal boundary conditions is straightforward. The irreversibility associated with the Second Law of Thermodynamics is an automatic unavoidable consequence of the multifractal attractors: Motions obeying the Law are stable, attracting nearby trajectories; motions violating the Law by lying near the inaccessible zero-volume fractal repeller are pushed away from this illegal structure by dynamical instability. Despite its simplicity, this mechanical approach may well seem overly simplistic to those who feel that deterministic boundaries are more “artificial” than stochastic ones. For these sceptics it seems specially paradoxical that the information dimension of occupied phase space is reduced away from equilibrium, in such a way that the Gibbs' entropy for the *complete* system, *including the boundaries*, diverges. In some cases, but not all, even the Hausdorff dimension, which characterizes the support of the attractor, has been shown to be nonintegral.^{2–5} It has not yet been possible to prove or disprove the conjecture that the Gibbs' entropy divergence still holds, after averaging over the boundary degrees of freedom, for the *projected distribution* of the bulk Newtonian degrees of freedom. If generally valid, such a divergence would rule out the use of nonequilibrium entropy in fundamental studies. On the other hand, Eyink and Lebowitz have suggested⁷ that the apparent conflict between multifractal distributions for deterministic boundaries and continuous distributions for stochastic boundaries might be resolved through an “approximately multifractal” distribution. The effect of boundaries on the Gibbs entropy is a promising research area. Lack of a decisive theoretical resolution suggests taking the alternative numerical approach, which we follow here.

But the numerical difficulties in analyzing many-body

distributions, so as to test and evaluate these ideas, are severe. It is true that modern computers make it possible to study the details of phase-space flows in spaces of up to several hundred dimensions, but accurate simulations then consume hundreds of hours of computer time. Thanks to parallel computers, this computational bottleneck is opening up⁸ relatively rapidly, but, because the computer time required increases at least as rapidly as the square of the number of particles (even with short-ranged interactions), present-day analyses necessarily reflect the fluctuations and surface effects inherent in small systems. In order to make the case for a multifractal attractor as clearly and simply as is possible, we here consider the number dependence of two of the simplest possible prototypical nonequilibrium flows, namely, a heat flow and a shear flow. For simplicity, both these systems are two dimensional.

The plan of the paper is as follows. In Sec. II we review the straightforward analysis leading to the general conclusion that nonequilibrium steady-state flows driven by deterministic boundaries inhabit (multi)fractal phase-space attractors. In Secs. III and IV we describe the two models, a four-chamber heat flow and a boundary-driven shear flow and present numerical results. Our conclusions make up the final section, Sec. V.

II. THEORY

In 1984 Shuichi Nosé introduced deterministic time-reversible equations of motion consistent with Gibbs' canonical ensemble.^{9,3} The "Nosé-Hoover" form of these equations incorporates friction coefficients $\{\xi\}$ capable of furnishing and withdrawing energy in such a way that, for an otherwise isolated system, Gibbs' canonical distribution, $f_N(q^N, p^N) \propto \exp[-H(q^N, p^N)/kT]$, can result. Whenever Nosé-Hoover deterministic thermostat forces $-\xi p$ are incorporated into the atomistic equations of motion for the "phase" $\Gamma \equiv \{q^N, p^N, \xi\}$:

$$\{\dot{q} = p/m; \dot{p} = F(q) - \xi p\}_N,$$

$$\dot{\xi} = [(p^2/\langle p^2 \rangle) - 1]/\tau^2 \equiv [(T/\langle T \rangle) - 1]/\tau^2,$$

the phase-space continuity equation (Liouville's Equation) relates the time-rate-of-change of the phase-space probability density, $f(q^N, p^N, \xi, t)$, and the comoving phase-space hypervolume, $\Theta(q^N, p^N, \xi, t)$, to the friction coefficients $\{\xi\}$, the Lyapunov exponents $\{\lambda\}$, and the externally produced entropy production \dot{S} :

$$\langle (d \ln f/dt) \rangle \equiv -\langle (d \ln \Theta/dt) \rangle \equiv -\Sigma \lambda \equiv +\langle \Sigma \xi \rangle \equiv \dot{S}/k.$$

The friction-coefficient sum $\Sigma \xi$ includes a term for each thermostatted momentum. The Lyapunov-exponent sum $\Sigma \lambda$ includes *all* the Lyapunov exponents. The *time average* $\langle \dots \rangle$ implies a *sufficiently long* time interval. Our numerical work on small systems ($N < 100$) indicates that a time of the order of ten thousand collision times is necessary for three-digit accuracy in the $\{\lambda\}$. Here, N indicates the number of bulk particles in the nonequilibrium flow, particles that interact with purely Newtonian forces.

In this paper we use D to represent the full dimensionality of the phase space, equal to the equilibrium value ($4N$ for N two-dimensional mass points, for instance) augmented by the additional nonequilibrium variables required to describe the boundary driving the flow. Thus a two-dimensional nine-body heat flow simulation with hot and cold temperatures T_H and T_C imposed by the friction coefficients ξ_H and ξ_C is described in a phase space of $D = 9 \times 4 + 2 = 38$ dimensions. In *any* nonequilibrium flow the phase-space volume shrinks with time, $(d \ln \Theta/dt) < 0$, establishing that the Lyapunov-exponent sum $\Sigma \lambda$ is negative while the mean value of the friction-coefficient sum $\langle \Sigma \xi \rangle \equiv -\Sigma \lambda$ is positive.

At *equilibrium* the complete spectrum of Lyapunov exponents is *symmetric*, a set of "Smale pairs," $\{\pm \lambda\}$. (This pairing^{10,11} follows from the time reversibility of the Hamiltonian equations of motion.) For a *large system* the first few exponents have similar values $\lambda_1 \approx \lambda_2 \approx \lambda_3$, as do also the last few, $-\lambda_3 \approx -\lambda_2 \approx -\lambda_1$. For a *driven system*, driven into a nonequilibrium steady state by Nosé-Hoover thermostats, the Nosé-Hoover equations of motion establish directly that the (negative) sum of *all* the Lyapunov exponents, $\Sigma \lambda \equiv -\langle \Sigma \xi \rangle$, is precisely equal to $-\dot{S}/k$, where \dot{S} is the external entropy production. Thus the *number of terms* required in a *vanishing partial sum* of exponents $\Sigma' \lambda$, with the sum of the *missing* (negative) terms, $\Sigma \lambda - \Sigma' \lambda$, equal to $-\dot{S}/k$, gives the (Kaplan-Yorke) information dimension of the lower dimensional (lower than the phase-space dimension D by ΔD , the number of missing terms) strange attractor. The criterion of a vanishing sum of exponents is a natural one. Phase-space objects with fewer dimensions than $D - \Delta D$ must grow in time, while those with higher dimensionality must shrink.

It is relatively easy to make a qualitative estimate of the dimensionality reduction ΔD in the more general case, even far from equilibrium. In *dense fluids* the shear viscosity coefficient is of order $m\nu/\sigma$, where ν and σ are the collision frequency and collision diameter, respectively. If we also use the collision frequency as a rough estimate for the Lyapunov exponent, $\nu \approx \lambda_1$, then a *shear flow* with strain-rate $\dot{\epsilon}$ should display a drop of dimensionality of order $\Delta D/D \approx (\sigma \dot{\epsilon}/c)^2$, where $c \approx \nu \sigma$ is the speed of sound. Likewise, the corresponding dimensionality drop for a *heat flow* driven by a temperature gradient ∇T is $\Delta D/D \approx (\sigma \nabla T/T)^2$. Despite these promising estimates, until now numerical estimates of the drop in phase-space dimensionality were typically no greater than 4 or 5 in boundary-driven shear flows.¹⁰ In those cases investigated so far, the decrease of the most-negative Lyapunov exponents has been much greater than $-\Sigma \lambda/D$, leading to a relatively smaller decrease in dimensionality. Only in one simulation did the drop marginally exceed 5. In that case, the drop was only 5.09 ± 0.015 . As explained in Sec. IV, 5 was mistakenly thought to be the additional number of coordinates required to describe the nonequilibrium flow. Although statistically significant, the borderline nature of this result fueled the suspicion that boundary-driven flows retain, at the least, the full dimensionality of the equilibrium phase space. We have therefore undertaken here to explore the

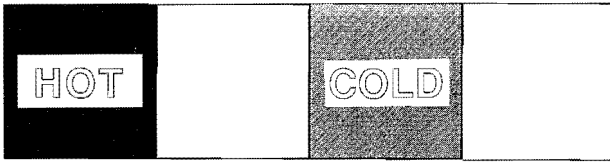


FIG. 1. Periodic four-chamber system composed of hot and cold reservoir regions interacting with two Newtonian regions. All particles are treated identically, and can move freely among the four regions, obeying equations of motion without friction in the Newtonian chambers, and with hot or cold friction coefficients ξ_H or ξ_C within the two reservoir chambers.

dimensionality drop in more detail than was possible in our earlier work.

In the work described here, we began by investigating lower density flows. At low density both the kinematic viscosity coefficient and the thermal diffusivity are of order $c\lambda_{\text{MFP}}$, where c is the speed of sound and λ_{MFP} is the mean free path. An intuitive low-density estimate for the Lyapunov exponent is $\lambda_1 \approx c/\lambda_{\text{MFP}}$, leading to predicted attractor dimensionality reductions $\Delta D/D = (\lambda_{\text{MFP}}\dot{\epsilon}/c)^2$ and $(\lambda_{\text{MFP}}\nabla T/T)^2$. Despite these predictions exploratory numerical low-density simulations were not encouraging. Again, the most negative Lyapunov exponents show relatively large shifts. These empirical tests led us to reinvestigate the more-favorable high-density situation.

III. HEAT-FLOW MODEL

Consider a *periodic* two-dimensional system divided up into four equal parts, as is shown in Fig. 1. Within the “hot” and “cold” thermostatted regions the [Nosé-Hoover] equations of motion are

$$m\dot{r} = p; \quad \dot{p} = F - \xi_T p;$$

$$\dot{\xi}_T = [p_x^2 + p_y^2 - 2mkT_T]/(2mkT_T\tau^2),$$

with the subscript T equal to H or C , for hot or cold, and indicating the temperature. In the two Newtonian regions adjacent to these reservoir regions the thermostat forces involving the friction coefficients, ξ_H or ξ_C , are absent and the equations of motion are Newton's

$$m\ddot{r} \equiv \dot{p} \equiv F(r).$$

For the heat-flow system shown in Fig. 1 the complete phase-space description depends upon the $4N$ fluid coordinates $\{x, y, p_x, p_y\}_N$ together with the reservoir friction coefficients ξ_H and ξ_C characterizing the two heat reservoirs. Thus the N -body nonequilibrium phase space has $4N + 2$ dimensions.

In our numerical work we chose the colder temperature T_C , Boltzmann's constant k , the atomic mass m , as well as the products $2mkT_C\tau_C^2$ and $2mkT_H\tau_H^2$, all equal to unity. As usual,¹⁰ we used the specially smooth repulsive potential,

$$\phi(r < \sigma) = \epsilon[1 - (r/\sigma)^2]^4,$$

to generate collisional forces. In our numerical work we choose the energy ϵ equal to 100 and the length σ equal to 1. For kT set equal to 1, these choices correspond to a “collision diameter,” or “turning point,” $r = 0.8\sigma$.

We have used Benettin's method¹² to calculate complete Lyapunov spectra for systems with one, four, and nine particles in each of the square regions. For this, we follow the motion of a reference trajectory as well as $4N + 2$ orthonormal phase-space offset vectors $\{\delta\}$ giving the locations of $4N + 2$ “satellite” trajectories infinitesimally displaced from the “reference” trajectory $\Gamma_{\text{REF}}\{x, y, p_x, p_y, \xi_H, \xi_C\}$, where all the variables shown in braces depend upon the time. A typical $4N + 2$ -dimensional offset vector $\delta_i \equiv \{\delta x, \delta y, \delta p_x, \delta p_y, \delta \xi_H, \delta \xi_C\}_i$ obeys the unconstrained equations of motion:

$$\dot{\delta}_i = D \cdot \delta_i,$$

and is simultaneously constrained to remain orthonormal to the other vectors $\delta_{i+1}, \delta_{i+2}, \dots$, by Gram-Schmidt orthonormalization, carried out at every time step. In 1985 we developed an alternative more-elegant Lagrange-multiplier approach for imposing these constraints, but, for the relatively large systems of equations considered here, we have adopted the Gram-Schmidt approach to reduce the numerical work.

The square symmetric dynamical matrix D gives the derivatives of the equations of motion with respect to the phase-space coordinates, $D \equiv \partial\dot{\Gamma}/\partial\Gamma$. In this paper we use san serif type to distinguish the matrix D from the phase-space dimensionality D . D can be expressed equivalently in terms of the motion of the offset vectors, $D \equiv \partial\dot{\delta}/\partial\delta$. In the heat-flux problem the accelerations depend upon both particle and boundary coordinates as well as on the friction coefficients ξ_H and ξ_C , so that the matrix D contains *all* the corresponding derivatives. A sampling of nonvanishing matrix elements is as follows:

$$\frac{\partial \dot{x}}{\partial p_x} = \frac{1}{m}; \quad \frac{\partial \dot{y}}{\partial p_y} = \frac{1}{m};$$

$$\frac{\partial \dot{p}_x}{\partial x} = -\phi_{xx}; \quad \frac{\partial \dot{p}_x}{\partial y} = -\phi_{xy};$$

$$\frac{\partial \dot{p}_y}{\partial x} = -\phi_{xy}; \quad \frac{\partial \dot{p}_y}{\partial y} = -\phi_{yy};$$

$$\frac{\partial \dot{\xi}}{\partial p_x} = \frac{p_x}{mkT\tau^2}; \quad \frac{\partial \dot{\xi}}{\partial p_y} = \frac{p_y}{mkT\tau^2},$$

equivalent to the equations of motion:

$$\frac{\partial \delta \dot{x}}{\partial \delta p_x} = \frac{1}{m}; \quad \frac{\partial \delta \dot{y}}{\partial \delta p_y} = \frac{1}{m};$$

$$\frac{\partial \delta \dot{p}_x}{\partial \delta x} = -\phi_{xx}; \quad \frac{\partial \delta \dot{p}_x}{\partial \delta y} = -\phi_{xy};$$

$$\frac{\partial \delta \dot{p}_y}{\partial \delta x} = -\phi_{xy}; \quad \frac{\partial \delta \dot{p}_y}{\partial \delta y} = -\phi_{yy};$$

TABLE I. Phase-space dimensionality reduction (rounded to the nearest integer) ΔD for N two-dimensional atoms in a periodic box composed of a hot square, at temperature T_H , a Newtonian square, a cold square at temperature $T_C \equiv 1$ and a second Newtonian square; see Fig. 1. Periodic boundaries are imposed in both directions. The total area is N . The data are all based on 10 000-step simulations with a timestep equal to 0.001. The total number of Lyapunov exponents exceeds the equilibrium number by 5: $D = 4N + 5$. Particle mass, Boltzmann's constant, and the two reservoir products $2mkT\tau^2$ are all taken equal to unity. The pair potential is $\phi(r < \sigma) \equiv \phi(r < 1) \equiv \epsilon[1 - (r/\sigma)^2]^4 \equiv 100[1 - r^2]^4$.

N	kT_H	D	ΔD
4	4	21	1
16	4	69	2
36	4	149	3
36	9	149	9
36	16	149	21

$$\frac{\partial \delta \dot{\zeta}}{\partial \delta p_x} = \frac{p_x}{mkT\tau^2}, \quad \frac{\partial \delta \dot{\zeta}}{\partial \delta p_y} = \frac{p_y}{mkT\tau^2},$$

where the subscripts in the expressions ϕ_{xx} , ϕ_{xy} , and ϕ_{yy} indicate corresponding second derivatives of the pair potential.

We have used both the classic fourth-order Runge-Kutta method and a generalization of Störmer's method to integrate the system of $(4N + 2)(4N + 3)$ coupled ordinary differential equations corresponding to one reference and $4N + 2$ satellite trajectories. The number of ordinary differential equations to be solved ranges from 342 (for four particles) to 21 462 (for 36 particles). Despite fluctuations in the individual Lyapunov exponents the phase-space attractor dimensionality stabilizes relatively quickly.

Results are given in Table I. We show the reduction in the Kaplan-Yorke phase-space dimensionality ΔD computed from the Lyapunov spectrum. The reduction is only a few, for small systems, but becomes a relatively large fraction of the total phase-space dimension for systems with a few dozen degrees of freedom. It is clear that the reduction can easily exceed the two extra phase-space coordinates ζ_x and ζ_y required by the thermostats. But because roughly half the particles occupy the two thermostatted regions at any time it cannot be said that this reduction necessarily involves the dynamics of particles obeying Newton's equations of motion. The maximum dimensionality reduction shown in the table, $\Delta D = 21$ for a 36-particle system, is considerably less than the 72 Lyapunov exponents associated with half the total number of particles.

In addition to the simulations described here and listed in Table I, we also carried out a less-extensive investigation of heat flow with each of the two reservoir regions replaced by a single (planar) degree of freedom. Thus the $4N$ Newtonian phase-space coordinates $\{x_i, y_i, p_{x_i}, p_{y_i}\}_N$ were augmented by the six driving coordinates $\{X_H, P_{x_H}, \zeta_H, X_C, P_{x_C}, \zeta_C\}$. In all of the corresponding simulations the reduction in phase-space dimensionality ΔD failed to exceed 6, the number of additional phase-space coordinates required for thermal driving.

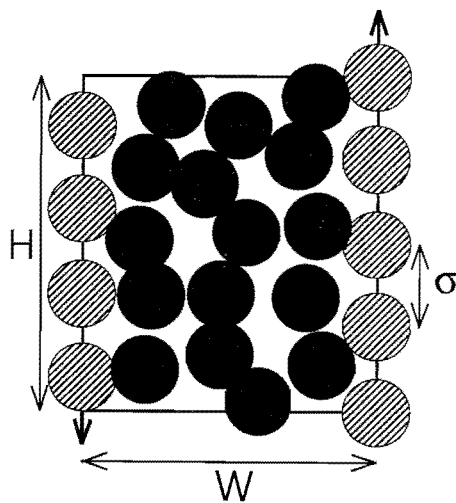


FIG. 2. Sixteen-particle system with width $W = 3.5$ and height $H = 4$. The corresponding total instantaneous phase-space dimension is $16 \times 4 + 5 = 69$. Newtonian particles are shown in black. Their motion is driven by the moving periodic corrugated boundaries, each made up of four moving particles (shaded). The top and bottom boundaries are periodic. The (moving) vertical boundaries include both smooth repulsive interactions $\phi(r) \equiv \epsilon[1 - (r/\sigma)^2]^4 \equiv 100[1 - r^2]^4$ and impulsive elastically reflecting barriers which prevent the escape of particles from the system. The time-periodic nature of the relative vertical boundary displacement corresponds to a total time-averaged phase-space dimension of $69 + 1 = 70$.

IV. SHEAR-FLOW MODEL¹⁰

Now consider a two-dimensional fluid, periodic in the vertical y direction and bounded in the x direction by two vertical moving corrugated isothermal walls, as shown in Fig. 2. In the horizontal direction the two walls move together so that the system's wall-center-to-wall-center width, $x_{\text{RIGHT}} - x_{\text{LEFT}} \equiv W$, is constant. Thus the $4N$ fluid coordinates $\{x_i, y_i, p_{x_i}, p_{y_i}\}_N$ are augmented by the set of two wall coordinates, two momenta, and a single friction coefficient ζ characterizing the boundary $\{X, Y, P_x, P_y, \zeta\}$. In addition to these $4N + 5$ variables, the vertical displacement (y direction) of the right-hand boundary particles relative to the left-hand ones is periodic in *time*, with a period $\sigma/(W\dot{\epsilon})$, or equivalently periodic in the apparent shear strain ϵ , with a maximum strain σ/W , where $\dot{\epsilon}$ is the strain rate du_y/dx and the strain $0 < \epsilon < (\sigma/W)$ measures the apparent vertical displacement of the right-hand boundary wall relative to that of the left-hand wall. Thus, including an extra phase-space time dimension, or the equivalent strain dimension, the *complete* nonequilibrium phase space contains $4N + 6$ dimensions. In our earlier work with this model,¹⁰ we overlooked the presence of this additional dimension.

The equations of motion of all N particles enclosed by the boundary are Newtonian, $\{m\ddot{r} \equiv \dot{p} \equiv F(r)\}_N$, while the equations of motion for the (two) boundary degrees of freedom, $\{X, Y\}$, follow the Nosé-Hoover form, and incorporate the macroscopic strain rate $\dot{\epsilon} \equiv du_y/dx$:

$$m\dot{X} = P_x; \quad m\dot{Y} = \pm [mW\dot{\epsilon}/2] + P_y;$$

$$\dot{P}_x = F_x - \zeta P_x; \quad \dot{P}_y = F_y - \zeta P_y;$$

$$\dot{\zeta} = [P_x^2 + P_y^2 - 2mkT]/(2mkT\tau^2).$$

$$\frac{\partial \dot{p}_y}{\partial X} = -\frac{\partial \dot{p}_y}{\partial x}; \frac{\partial \dot{p}_y}{\partial Y} = -\frac{\partial \dot{p}_y}{\partial y},$$

$$\frac{\partial \dot{\zeta}}{\partial P_x} = \frac{P_x}{mkT\tau^2}; \frac{\partial \dot{\zeta}}{\partial P_y} = \frac{P_y}{mkT\tau^2}.$$

The forces F_x and F_y in these boundary equations of motion are vector sums of the interactions of all N -Newtonian particles with the $2(H/\sigma)$ rigidly connected centers of force which make up the boundary, as is shown in Fig. 2. In order to avoid the escape of Newtonian particles through the moving boundaries, we added an additional short-ranged Lennard–Jones repulsive boundary interaction, $4\epsilon[(\sigma_{LJ}/r)^{12} - (\sigma_{LJ}/r)^6]$ for $r < 2^{1/6}\sigma_{LJ}$, with a characteristic length σ_{LJ} equal to $\sigma/10$.

For simplicity, we again use the same mass $m \equiv 1$ for all degrees of freedom, including the total mass associated with the two boundary degrees of freedom. Again Boltzmann's constant k is set equal to unity and, just as before, we use the specially smooth repulsive potential

$$\phi(r < \sigma) = \epsilon[1 - (r/\sigma^2)]^4 \equiv 100[1 - r^2]^4$$

to generate collisional forces.

We began by calculating complete Lyapunov spectra for square systems with $N = 4, 16, 25, 36,$ and 49 Newtonian particles at a variety of strain rates and densities. We turned later to nonsquare systems with from $4 \times 3 = 12$ to $4 \times 24 = 96$ bulk Newtonian particles. In every case we followed the motion of $4N + 5$ orthonormal phase-space offset vectors $\{\delta\}$ giving the locations of $4N + 5$ "satellite" trajectories infinitesimally displaced from the "reference" trajectory $\{x, y, p_x, p_y, X, Y, P_x, P_y, \zeta\}$. A typical $4N + 5$ dimensional offset vector $\delta_i \equiv \{\delta x, \delta y, \delta p_x, \delta p_y, \delta X, \delta Y, \delta P_x, \delta P_y, \delta \zeta\}_i$ obeys the unconstrained equations of motion:

$$\dot{\delta}_i = D \cdot \delta_i,$$

and is simultaneously constrained to remain orthonormal to the other vectors $\delta_{i+1}, \delta_{i+2}, \dots$, by Gram–Schmidt orthonormalization. Just as in our heat-flow example, we have adopted Bennetin's Gram–Schmidt approach to reduce the numerical work in analyzing our high-dimensional attractors.

As usual, the dynamical matrix giving the motion of the offset vectors is a square matrix. It should be noted that the accelerations depend upon both particle and boundary coordinates as well as on the friction coefficient ζ , so that the matrix D contains all the corresponding derivatives. A sampling of nonvanishing matrix elements is as follows:

$$\frac{\partial \dot{x}}{\partial p_x} = \frac{1}{m}; \frac{\partial \dot{y}}{\partial p_y} = \frac{1}{m};$$

$$\frac{\partial \dot{X}}{\partial P_x} = \frac{1}{m}; \frac{\partial \dot{Y}}{\partial P_y} = \frac{1}{m};$$

$$\frac{\partial \dot{p}_x}{\partial x} = -\phi_{xx}; \frac{\partial \dot{p}_x}{\partial y} = -\phi_{xy};$$

$$\frac{\partial \dot{p}_y}{\partial x} = -\phi_{xy}; \frac{\partial \dot{p}_y}{\partial y} = -\phi_{yy};$$

$$\frac{\partial \dot{p}_x}{\partial X} = -\frac{\partial \dot{p}_x}{\partial x}; \frac{\partial \dot{p}_x}{\partial Y} = -\frac{\partial \dot{p}_x}{\partial y};$$

For simplicity, we used the classic fourth-order Runge–Kutta method to integrate the system of $(4N + 5)(4N + 6)$ coupled ordinary differential equations, so that the number of equations solved ranged from $462 = 21 \times 22$ (for four particles plus boundary) to $151\,710 = 389 \times 390$ (for 96 particles and the boundary). For comparison we carried out a number of simulations using a generalized Störmer method. There was no significant dependence of the results on the method of integration.

We began by considering variations about an initial state with the number density set equal to 1, the relaxation time τ set to $1/4$, and the strain rate $\dot{\epsilon}$ to 1. Short trial-and-error runs indicated that higher densities and slightly faster relaxation times led to a greater reduction in dimensionality. Typical results are listed in Table II. For *most* of these simulations the reduction in dimensionality exceeds 5. For *some* of them the reduction exceeds 6 and approaches 7.

The data demonstrate conclusively that the instantaneous (or equivalently, *fixed-strain*) phase-space probability density for a 16-body system, with 64 Newtonian phase-space coordinates, confined to a rectangular box with dimensions 3.5×4 , and driven by five additional boundary coordinates $\{X, Y, P_x, P_y, \zeta\}$, can have a Kaplan–Yorke dimension considerably less than the maximum possible Newtonian contribution of 64. To illustrate this point, let us consider the results of a careful computation, involving 500 000 timesteps of 0.001 each, at a strain rate of 2 and with a relaxation time τ of 0.25. The simulations were carried out in the 69-dimensional phase space, in which the dimensionality decrease ΔD was 5.52. Because the additional Lyapunov exponent associated with the missing time, or strain, dimension is identically zero the same dimensionality decrease ΔD must apply also in the full 70-dimensional phase space. The resulting attractor dimension is therefore 64.48 ± 0.03 in the 70-dimensional space. The phase space describing a fixed time or strain is analogous to the two-dimensional Poincaré sections used to characterize three-dimensional dynamical systems. In the 69-dimensional phase space of the calculation, at a fixed time or fixed strain, the corresponding instantaneous attractor dimension is 63.48, *less than 64*, the Newtonian contribution. For larger systems even the *time-averaged* (averaged over time or strain) probability density inhabits a space with dimensionality less than the equilibrium dimensionality of $4N$. The maximum reduction in Table II, $\Delta D = 6.79$ indicates a time-averaged attractor dimension lying below the time-independent dimension by 0.79. The instantaneous attractor lies below the equilibrium dimension by 1.79 in this case. We expect to be able to achieve reductions exceeding 7 by further increasing the system size.

TABLE II. Sample values of phase-space dimensionality reduction ΔD for N two-dimensional atoms in a periodic box with a thermostatted moving boundary. The strain rate $(\dot{y}_{\text{RIGHT}} - \dot{y}_{\text{LEFT}})/W$ and the relaxation time τ are listed. All masses are unity. The height of the box (see Fig. 2) is $H/\sigma = H$ and the width is $W/\sigma = W$; N is the number of Newtonian particles. The boundary temperature is T . Periodic boundaries are imposed in the vertical direction. All the data are based on runs with a maximum time of at least 200 using the indicated value of the timestep dt . The total number of Lyapunov exponents is $D = 4N + 6$, with the extra six exponents corresponding to the two boundary coordinates, the two boundary momenta, the boundary friction coefficient, and the relative phase of the vertical boundary displacements. The pair potential is $100[1 - (r/\sigma)^2]^4 = 100[1 - r^2]^4$ for $r < 1$. The statistical uncertainty of the ΔD data is estimated at ± 0.03 .

$\dot{\epsilon}$	τ	N	H	W	kT	dt	ΔD
2.0	0.01	12	3.0	3.5	1.0	0.001 ^a	4.06
2.0	0.02	12	3.0	3.5	1.0	0.002 ^a	4.74
2.0	0.03	12	3.0	3.5	1.0	0.002 ^a	5.27
2.0	0.04	12	3.0	3.5	1.0	0.002 ^a	5.48
2.0	0.0625	12	3.0	3.5	1.0	0.001 ^a	5.70
2.0	0.10	12	3.0	3.5	1.0	0.001 ^a	5.76
2.0	0.25	12	3.0	3.5	1.0	0.001 ^a	5.57
2.0	0.01	16	4.0	3.5	1.0	0.001 ^a	4.35
2.0	0.02	16	4.0	3.5	1.0	0.002 ^a	5.08
2.0	0.03	16	4.0	3.5	1.0	0.002 ^a	5.50
2.0	0.04	16	4.0	3.5	1.0	0.002 ^a	5.68
2.0	0.0625	16	4.0	3.5	1.0	0.001 ^b	5.7
2.0	0.0625	16	4.0	3.5	1.0	0.001 ^a	5.74
2.0	0.0625	16	4.0	3.5	1.0	0.005	5.7
2.0	0.10	16	4.0	3.5	1.0	0.001 ^a	5.70
2.0	0.25	16	4.0	3.5	1.0	0.001 ^a	5.52
2.0	0.25	16	4.0	5.0	0.25	0.01	3.3
2.0	0.25	16	4.0	5.0	1.0	0.001 ^a	5.09
2.0	0.25	16	4.0	5.0	4.0	0.01	2.1
2.0	0.25	16	8.0	9.0	1.0	0.001 ^a	0.86
2.0	0.25	16	12.0	13.0	1.0	0.001 ^a	0.60
2.0	1.00	16	4.0	3.5	1.0	0.01	5.5
2.0	0.01	24	6.0	3.5	1.0	0.001 ^a	4.74
2.0	0.02	24	6.0	3.5	1.0	0.002 ^a	5.47
2.0	0.03	24	6.0	3.5	1.0	0.002 ^a	5.77
2.0	0.04	24	6.0	3.5	1.0	0.001 ^a	5.86
2.0	0.0625	24	6.0	3.5	1.0	0.001 ^a	5.80
2.0	0.10	24	6.0	3.5	1.0	0.001 ^a	5.60
2.0	0.25	24	6.0	3.5	1.0	0.001 ^a	5.50
2.0	0.25	25	5.0	3.0	1.0	0.001	5.5
2.0	0.25	25	5.0	4.2	1.0	0.002	5.4
2.0	0.25	25	5.0	6.0	1.0	0.01	4.9
4.0	0.25	25	5.0	6.0	1.0	0.0025	2.6
4.0	0.25	25	5.0	6.0	1.0	0.001	2.6
2.0	0.25	30	6.0	7.0	1.0	0.001	5.0
2.0	0.01	32	8.0	3.5	1.0	0.001 ^a	5.16
2.0	0.02	32	8.0	3.5	1.0	0.002 ^a	5.78
2.0	0.03	32	8.0	3.5	1.0	0.002 ^a	5.93
2.0	0.04	32	8.0	3.5	1.0	0.002 ^a	6.01
2.0	0.0625	32	8.0	3.5	1.0	0.001 ^a	5.83
2.0	0.10	32	8.0	3.5	1.0	0.002 ^a	5.60
2.0	0.25	32	8.0	3.5	1.0	0.002 ^a	5.49
2.0	0.01	48	12.0	3.5	1.0	0.002 ^a	5.65
2.0	0.02	48	12.0	3.5	1.0	0.002 ^a	6.14
2.0	0.03	48	12.0	3.5	1.0	0.002 ^a	6.25
2.0	0.04	48	12.0	3.5	1.0	0.002 ^a	6.20
2.0	0.0625	48	12.0	3.5	1.0	0.002 ^a	5.93
2.0	0.10	48	12.0	3.5	1.0	0.002 ^a	5.75
2.0	0.25	48	12.0	3.5	1.0	0.002 ^a	5.65
2.0	0.01	60	15.0	3.5	1.0	0.002 ^a	6.00
2.0	0.02	60	15.0	3.5	1.0	0.002 ^a	6.35
2.0	0.03	60	15.0	3.5	1.0	0.002	6.39
2.0	0.04	60	15.0	3.5	1.0	0.002 ^a	6.29
2.0	0.0625	60	16.0	3.5	1.0	0.002 ^a	5.99
2.0	0.10	60	16.0	3.5	1.0	0.002	5.83
2.0	0.25	60	16.0	3.5	1.0	0.002	5.72

TABLE II. (Continued.)

$\dot{\epsilon}$	τ	N	H	W	kT	dt	ΔD
2.0	0.01	96	24.0	3.5	1.0	0.002	6.63
2.0	0.02	96	24.0	3.5	1.0	0.002	6.79
2.0	0.03	96	24.0	3.5	1.0	0.002	6.73
2.0	0.04	96	24.0	3.5	1.0	0.002	6.45
2.0	0.0625	96	24.0	3.5	1.0	0.002	6.25

^aRun up to at least $t_{\max} = 500$.

^bThe Lyapunov spectrum from this run is displayed in Fig. 3.

The complete spectrum of the $70 - 3 = 67$ nonvanishing Lyapunov exponents for a typical 200 000-step simulation described in Table II, is shown in Fig. 3. Three of the Lyapunov exponents vanish, in the 70-dimensional space, reflecting the lack of relative motion in three phase-space directions. One such direction corresponds to the trajectory direction in that space. This reflects the observation that two phase-space points separated by a fixed time interval δt have no tendency to separate as time goes on. Likewise, the absolute location of the system in space can have no effect on the motion. Because the Nosé-Hoover frictional forces operating at the boundary do not conserve momentum it is possible for the center-of-mass of the system to drift in space. There are thus two more vanishing exponents corresponding to the absolute (x, y) location of the system.

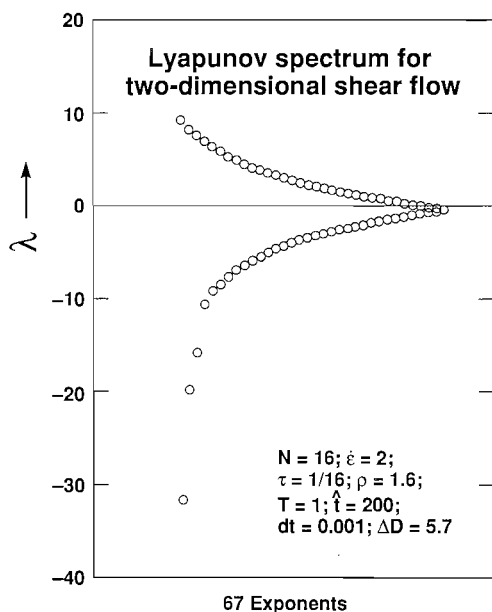


FIG. 3. Lyapunov spectrum for a 16-body nonequilibrium steady state of the type shown in Fig. 2, showing an instantaneous attractor dimension significantly less than that of the Newtonian degrees of freedom. The data are averages over 200 000 timesteps of length 0.001. The 67 nonvanishing exponents are plotted as pairs $\{\lambda_i, \lambda_{68-i}\}$ equally spaced in the abscissa direction. Note that the Smale-pair symmetry is broken away from equilibrium and that the number of nonvanishing exponents is odd despite the time-reversal symmetry of the equations of motion.

V. CONCLUSIONS

This work illustrates the reduction of phase-space attractor dimension inherent in irreversible deterministic phase-space flows. We find quantitative results which are insensitive to the method of integration and the timestep.

At low density, which theoretical considerations suggest would be the most favorable case, there is a tendency for particles to clump near the boundaries, reducing both the momentum transport and the reduction in phase-space dimensionality. This effect could possibly be eliminated by using a more complicated boundary with, for example, even and odd boundary particles undergoing thermal displacements in opposite directions.

In many cases, even with a relatively small number of particles, the instantaneous reduction in dimensionality exceeds the added dimensionality required to drive the system from equilibrium. But the reduction of the attractor dimension seems to be limited, at least for the system sizes we could study, to reductions which are only a bit larger than the added phase-space dimensionality. Roughly, the maximum decrease ΔD seems to vary as $\ln N$. Nevertheless, these results do establish conclusively that both the instantaneous and the boundary-phase-averaged distribution functions for the Newtonian degrees of freedom can actually be multifractal objects and can therefore correspond to a divergent Gibbs entropy. Of course, reduced distribution functions, obtained by integrating $f(q, p, \xi, \epsilon)$ over a subset of the phase-space coordinates, are subspace projections describing the correlations of fewer coordinates or momenta and do not share this fractal character. It is most interesting to see that dissipative boundary degrees of freedom can act to reduce the phase-space dimensionality of purely Newtonian systems with which they interact.

Despite the characteristic large shifts of the most-negative Lyapunov exponents, noted before¹⁰ in our less extensive investigation, it has here been shown that both the time-averaged and instantaneous attractor dimensions can lie well below the corresponding Newtonian equilibrium dimensions. We must emphasize that we cannot prove that this reduction in information dimension, below the Newtonian value, occurs for larger systems. We cannot prove that there is an intrinsic reduction independent of the boundary conditions. The results cited in Ref. 7 indicate that no completely general conclusion can be reached, at least for small systems. If the dimensionality reduction were to persist for large systems, as we believe is likely, the

implications would be fundamental for nonequilibrium statistical mechanics. In this case there would be no possibility to use Gibbs' entropy in discussing general nonequilibrium systems. Although a comprehensive proof is still lacking, we wish to emphasize that the nonequilibrium heat-reservoir techniques used here are exactly consistent with the transport coefficients predicted by near-equilibrium Green-Kubo linear response theory^{3,11,13} and with the flow directions predicted by the far-from-equilibrium Second Law of Thermodynamics. This agreement supports our view that the deterministic time-reversible Nosé-Hoover equations of motion are uniquely well suited to the study of nonequilibrium systems. To establish that the dimensionality reduction found here is typical of the general situation, beyond reasonable doubt, requires either a theoretical breakthrough or further more-decisive brute-force studies of the size dependence and the boundary dependence of nonequilibrium flows. As massively parallel computation becomes commonplace, it will become possible to extrapolate our results to somewhat larger systems and to carry out studies with other boundary conditions so as to determine the universal properties of large-system fractal dimensionality.

VI. ACKNOWLEDGMENTS

This work was inspired by conversations and discussions at the 1991 NATO Advanced Study Institute, "Simulation of Complex Hydrodynamic Flows," held near Alghero, Sardinia, Italy and organized by Michel Mareschal and Brad Holian. We specially thank Joel Lebowitz, Greg Nicolis, and Eddie Cohen for their dogged insistence that the phase-space reduction be demonstrated. Joel Lebowitz and Gregory Eyink thoughtfully commented at length on the finished manuscript and were responsible for its subsequent revisions. Brad Holian's advice and perceptive comments, both before and after a first draft of this work, were very helpful. We would like to thank the National Science Foundation for generous travel support. In Vienna this work was supported by the Austrian Fonds zur Foerd-

erung der Wissenschaftlichen Forschung, Grant P8003, and by the Computer Center of the University of Vienna, operating within the framework of IBM's European Supercomputer Initiative. In Livermore work was carried out under the auspices of the United States Department of Energy by the Lawrence Livermore National Laboratory.

¹B. L. Holian, W. G. Hoover, and H. A. Posch, *Phys. Rev. Letts.* **59**, 10 (1987); W. G. Hoover, *Phys. Rev. A* **37**, 252 (1988).

²H. A. Posch, W. G. Hoover, and B. L. Holian, *Ber. Bunsen Ges. Für Phys. Chem.* **94**, 250 (1990).

³W. G. Hoover, *Computational Statistical Mechanics* (Elsevier, Amsterdam, 1991).

⁴B. Moran, W. G. Hoover, and S. Bestiale, *J. Stat. Phys.* **48**, 709 (1987).

⁵W. G. Hoover, C. G. Hoover, W. J. Evans, B. Moran, J. A. Levatin, and E. A. Craig, in the Proceedings of a NATO workshop *Microscopic Simulations of Complex Flows*, edited by M. Mareschal held 23-25 August 1989 in Brussels (Plenum, New York, 1990), p. 199.

⁶See, for instance, M. Mareschal, "Microscopic Simulations of Instabilities," in *Microscopic Simulations of Complex Flows*, NATO Advanced Study Institute, Series B: Physics, Volume 236, edited by M. Mareschal (Plenum, New York, 1990), p. 141 as well as D. Kusnezov, A. Bulgac, and W. Bauer, *Ann. Phys.* **204**, 155 (1990).

⁷See the discussion remarks in *Simulation of Complex Hydrodynamic Flows*, the Proceedings of a NATO Advanced Science Institute held 13-26 July 1991 in Sardinia, Italy (Plenum, New York, 1992). We thank Gregory Eyink and Joel Lebowitz (many private communications, 1991 and 1992) for describing rigorous results for systems with stochastic boundaries and emphasizing the relevance of those results to our own work. The rigorous results are contained in two references: W. Goldstein, C. Kipnis, and N. Ianiro, *J. Stat. Phys.* **41**, 915 (1985); S. Goldstein, J. L. Lebowitz, and E. Presutti, *Colloquia Math. Soc. Janos Bolyai* **27**, *Random Fields* (Esztergon, Hungary, 1981).

⁸A. J. De Groot, E. M. Johansson, J. P. Fitch, C. W. Grant, and S. R. Parker, *IEEE Trans. Nucl. Sci.* **34**, 873 (1987).

⁹S. Nosé, *J. Chem. Phys.* **81**, 511 and *Mol. Phys.* **52**, 255 (1984); W. G. Hoover, *Phys. Rev. A* **31**, 1695 (1985).

¹⁰H. A. Posch and W. G. Hoover, *Phys. Rev. A* **38**, 473 (1988); *A* **39**, 2175 (1989).

¹¹D. J. Evans, E. G. D. Cohen, and G. P. Morriss, *Statistical Mechanics of Nonequilibrium Liquids* (Academic, London, 1990).

¹²G. Benettin, L. Galgani, and J. Strelcyn, *Phys. Rev. A* **14**, 2338 (1976); W. G. Hoover and H. A. Posch, *Phys. Letters A* **123**, 227 (1987); W. G. Hoover, C. G. Hoover, and H. A. Posch, *Physical Review A* **41**, 2999 (1990); G. P. Morriss, *Phys. Letters A* **134**, 307 (1989).

¹³See, for instance, W. G. Hoover, D. J. Evans, R. B. Hickman, A. J. C. Ladd, W. T. Ashurst, and B. Moran, *Phys. Rev. A* **22**, 1690 (1980).